*Journal of Experimental Botany, Vol. 55, No. 401, pp. 1423–1431, June 2004*
DOI: 10.1093/jxb/erh146 Advance Access publication 7 May, 2004

Journal of Experimental Botany

RESEARCH PAPER

# Combining thermal and visible imagery for estimating canopy temperature and identifying plant stress

**Ilkka Leinonen* and Hamlyn G. Jones**

*University of Dundee at SCRI, Plant Science Research Group, Invergowrie, Dundee DD2 5DA, Scotland, UK*

Received 17 February 2004; Accepted 20 March 2004



## Abstract

**Thermal imaging is a potential tool for estimating plant temperature, which can be used as an indicator of stomatal closure and water deficit stress. In this study, a new method for processing and analysing thermal images was developed. By using remote sensing software, the information from thermal and visible images was combined, the images were classified to identify leaf area and sunlit and shaded parts of the canopy, and the temperature statistics for specific canopy components were calculated. The method was applied to data from a greenhouse water-stress experiment of *Vicia faba* L. and to field data for *Vitis vinifera* L. Vaseline-covered and water-sprayed plants were used as dry and wet references, respectively, and two thermal indices, based on temperature differences between the canopy and reference surfaces, were calculated for single *Vicia faba* plants. The thermal indices were compared with measured stomatal conductance. The temperature distributions of sunlit and shaded leaf area of *Vitis vinifera* canopies from natural rainfall and irrigation treatments were compared. The present method provides two major improvements compared with earlier methods for calculating thermal indices. First, it allows more accurate estimation of the indices, which are consequently more closely related to stomatal conductance. Second, it gives more accurate estimates of the temperature distribution of the shaded and sunlit parts of canopy, and, unlike the earlier methods, makes it possible to quantify the relationship between temperature variation and stomatal conductance.**

Key words: Infrared thermography, remote sensing, stomatal conductance, *Vicia faba*, *Vitis vinifera*.

## Introduction

Remote sensing of stomatal closure and transpiration rates from plants has great potential as a tool for indicating irrigation need, and hence for improved crop management. For any given environmental conditions, the leaf or canopy temperature is directly related to the rate of evapotranspiration from the canopy surface. Therefore, infrared sensing of the canopy temperature can be used to monitor stomatal conductance or to estimate the transpiration rate of plants (Jackson, 1982; Jones, 1999*a*; Merlot *et al.*, 2002; Jones *et al.*, 2002).

The rate of evaporation is only one of many components of the canopy energy balance that affect canopy temperature: factors such as radiation, windspeed, air temperature, and air humidity also have major effects (Jones, 1992). Without sufficient information about these factors, measurements of leaf temperature alone are not enough to allow estimates of the transpiration rate or the stomatal conductance. One solution is to make use of 'dry' and 'wet' reference surfaces, where the observed leaf temperature is compared with the temperature that the same leaves would attain under the conditions of zero and maximum transpiration at the same environment (Jones *et al.*, 1997). The dry surface represents the situation without transpiration and the wet surface represents the maximum potential rate of transpiration. In earlier studies, some artificial reference surfaces were used, for example, wet and dry filter paper (Jones *et al.*, 2002). The problem, however, is that the thermal and radiative properties of these surfaces may differ from those of the observed plants, so that their energy balance differs from the real leaves. Therefore, Jones *et al.* (2002) proposed the use of leaves sprayed with water as wet references and leaves for which all transpiration was prevented by covering in petroleum jelly as dry references.

* To whom correspondence should be addressed. Fax: +44 (0)1382 562426. E-mail: i.leinonen@scri.sari.ac.uk

 

Throughout the 1970s and 1980s in particular, there was much effort on the development of thermal crop water-stress indices that could be used for irrigation scheduling purposes (Idso *et al.*, 1981; Idso, 1982; Jackson, 1982; see also Jones and Leinonen, 2003). These were based on the measurement of canopy temperature using infrared thermometers. A major problem with such measurements, however, is that it is common for the field of view of the detector to include some background (e.g. soil or sky) in addition to the leaves of the crop of interest, especially before full ground cover is achieved. One method for solving this problem was presented in an earlier study by Jones *et al.* (2002). They used wet and dry reference surfaces, located in a grapevine canopy, as thresholds, and all temperatures between these thresholds, occurring in the thermal image, were assumed to represent the temperature of the canopy.

As an alternative to the estimation of crop water stress from the mean temperature of the canopy, it has been proposed that the variability of canopy temperature may provide important information about the degree of stomatal closure (Fuchs, 1990). By contrast with infrared thermometry, thermal imaging allows information on the temperatures of all areas in a scene to be obtained simultaneously in one image. Therefore, thermal imagery provides an ideal approach for the collection of the large number of individual leaf temperatures that are necessary for methods based on temperature frequency distributions. Thermal imaging also allows leaves to be distinguished from the background. If done manually, however, the necessary image processing can be rather labour-intensive and may also be dependent on subjective image interpretation.

The present study outlines the development and testing of new automated approaches to the extraction of leaf temperatures from thermal images that are based on the combination of information from thermal and visible/near infrared images. Examples of the application of the method in greenhouse and field conditions are presented, including the extraction of temperature frequency distributions.

## Materials and methods

### Experimental material

*Greenhouse experiment*: The greenhouse experiment was carried out at the Scottish Crop Research Institute, Invergowrie, Scotland. In the experiment, broad bean (*Vicia faba* L.) seeds were sown on 7 April 2003 into 4" square pots. Compost was used as potting material. The temperature in the greenhouse was set to 23 °C for daytime and 18 °C for night-time. The daylength was 14 h and additional illumination was provided by sodium high pressure lamps. During the experiment, groups of plants were exposed to a drought stress of 2 d without water. The drought treatments for each experimental group were started on subsequent days, so at the time of the measurements (27 May), one group of seedlings had been exposed to a drought treatment for one day and one group for two days. In addition to the drought treatments, a control group of seedlings was watered daily.

Thermal and visual images were taken for ten plants from each treatment. The thermal images were taken for each plant separately with the SnapShot imager (see below) mounted on a tripod. In addition to the experimental plant, parts of two other plants were included in the image as dry and wet references. For the dry reference, the leaves of one branch were covered with Vaseline to prevent transpiration. The leaves of the wet reference plant were sprayed with water about 1 min before taking the image. Immediately after taking the thermal image, a visible image was taken by placing the Dycam Agricultural Digital Camera (see below) in front of the lens of the thermal imager, to make sure that both images were taken from the same angle.

*Field experiment*: The field measurements were conducted in July 2001 on mature grapevine (*Vitis vinifera* L. cvs Moscatel and Castelão (=Periquita)) leaves growing at the Portuguese Ministry of Agriculture Research Station at Pegões, Portugal (8° 40′ W; 38° 38′ 30" N). Details of the experiment are presented in Jones *et al.* (2002) and de Souza *et al.* (2003). The vineyard was 5-years-old and established on a deep sandy soil at 1 m spacing within the row and 2.5 m between rows. Each variety was grown in a different area of the field with a similar experimental design. There were four blocks of four irrigation treatments for each variety in a Latin square arrangement, with a single experimental row and two guard rows. The treatments used in this study were: NI (no irrigation) and FI (100% of $ET_C$ supplied through two trickle lines placed 20 cm each side of the row). The result of the treatment effects in this experiment have been presented earlier by Jones *et al.* (2002). In the present study, the data are used to test the method for estimating the canopy temperature.

### Ancillary measurements

Immediately after taking the thermal and visible images, the stomatal conductance of *Vicia faba* was measured using an AP4 porometer (Delta-T Devices, Burwell, Cambridge, England). Before the measurements, a standard calibration was carried out as indicated in the manual (Webb, 1990). A total of five leaves were measured for each plant. Environmental conditions (global and photosynthetically active radiation, air temperature, and relative humidity) in the greenhouse during the experiments were collected using DataHog (Skye Instruments, Llandidrod Wells) and DL2e (Delta-T Instruments, Burwell) data loggers. During the plant measurements, the interval of the data collection was 30 s and at other times during the experiment 10 min.

### Thermal and visible imaging

Thermal images were obtained with an Infrared Solutions SnapShot 225 long-wave (8–12 μm) thermal imager with a 20 mm (17.2° field of view) lens (supplied by Alpine Components, Oban Road, St Leonards-on-Sea, East Sussex, UK). The camera is a line-scan imager producing images of 120×120 pixels at 14 bit dynamic resolution, with corrections for object emissivity and background temperature. Emissivity was set at 0.95 for viewing leaves. The standard deviation of readings for individual pixels when measuring a constant temperature black background at room temperature was <0.35 °C. The *iFOV* or pixel size at closest focus (0.25 m) is 0.63 mm, increasing to 25.2 mm at 10 m. For corresponding visual images under greenhouse conditions, an Agricultural Digital Camera (Dycam, Woodland Hills, California, USA) was used. This provides two-colour images in the red and near infrared (R/NIR) that allows green plant material to be easily separated from background soil and most other materials on account of their very different reflectances in these two wavebands (Jones, 1992). Alternatively, a standard red/green/blue (RGB) digital camera can also be used, and data for the field experiment used a Canon digital Ixus instead of the Dycam instrument.

### *Image processing*

The objective is to separate the areas of interest (for example, leaves) from other objects included in the thermal image and to identify the temperature distributions of the selected areas. The main steps of this process are outlined in the following.

*Initial manipulation*: During continuous use of the thermal camera, internal warming caused a drift in the calibration of the camera resulting in a spatially varying error in the thermal images. These relative errors were corrected by using images of constant temperature background (out-of-focus images of the lens cap) as a reference (Jones *et al.*, 2002). Each pixel of the reference image was subtracted from the corresponding pixel of the actual image using the SnapView 2.1 software provided. Images were exported as ASCII text files for subsequent processing. The first step (in Microsoft Excel) was to add the mean temperature of the appropriate reference image back to each pixel in the subtracted image. This step was partly automated by building a Microsoft Excel macro for handling the data files.

*Overlaying images*: Further processing of the thermal images was carried out in the ENVI remote sensing software (Research Systems Inc., Boulder, Colorado) with the visible images in Bitmap format, and the corrected thermal images kept in text format. The thermal images may be viewed in ENVI in grey scale, where the brightness of each pixel indicates the measured temperature, or they may be viewed as pseudo-colour images if required.

In order effectively to combine the information from the thermal images and the visible images, it is essential that corresponding pixels can be identified from both types of images. In practice, this means that (i) both images must cover exactly the same area and (ii) the dimensions (and pixel sizes) of both images must be identical. In order to fulfil these criteria, the visible image was warped and resampled to overlay the thermal image exactly by using the Map function of the ENVI software. Corresponding Ground Control Points (GCPs) such as tips of leaves were selected manually from both the thermal and visible images. Because of the similar geometry of the two images, four points were generally sufficient for accurate overlaying of the images, especially if the points were spread evenly within the thermal image. Another option for image overlaying, made possible by the ENVI software, is to use preselected GCPs; this option would be useful for automation in cases where several images cover exactly the same area, for example, in studies of the dynamics of transpiration. After selecting the GCPs, the visible image was warped and resampled (using the Nearest Neighbour method) to match the thermal image using a Polynomial Warp (order=1). The dimensions of the warped image were selected to be identical to the thermal image (120×120 pixels).

*Classification*: Classification was performed using Supervised Classification in ENVI; for a detailed description of the principles of supervised classification see appropriate texts (Mather, 1999; Lillesand *et al.*, 2004). This involved initial manual identification of 'training areas' or Regions of Interest (ROIs) known to represent leaves in the visible image. The spectral information from these regions was then used to classify the visible image into pixels representing plant leaves (classified) and all other objects (unclassified), such as background and other non-green parts of the plant such as flowers. Similar classification procedures can be applied to separate different components of the area of interest further. For example, in the field study, the leaf class was further separated into sunlit and shaded areas, based on appropriate sunlit and shaded ROIs. If necessary, other ROIs, representing, for example, background, can also be selected for additional training classes. From different options available in the ENVI software, Spectral Angle Mapper and Minimum Distance methods were found to be most useful in this study. The Minimum Distance method determines the mean vector of the training areas and calculates the Euclidean distance of each unknown pixel to each of the mean training class values. Each pixel is classified to the nearest class, unless the distance is greater than the predetermined (optional) maximum distance, in which case the pixel remains unclassified. The Spectral Angle Mapper method calculates the vector angle between the spectra of training classes and each unknown pixel. Each pixel is classified to a training class for which the spectral angle between it and the pixel is the smallest. It is also possible to determine the maximum accepted angle between a classified pixel and a training class. If the calculated angle is greater, the pixel remains unclassified

In the case of the greenhouse data, the Spectral Angle Mapper method was applied since it requires only one training class (leaf area), and the classification can be done based on the maximum accepted vector angle only. Furthermore, compared with other classification methods, this method is relatively insensitive to changes in illumination (Lillesand *et al.*, 2004). However, in the case of the field data in this study, where the difference in the illumination of the leaves is one of the classification criteria, other methods, including Minimum Distance, are more suitable.

The classification step may be automated further by the use of ENVI Spectral Libraries. This would be useful in conditions where the spectral properties of the leaf area, for example, remain unchanged for a series of images. In practice, this means that the colour of the leaves or the light conditions do not change significantly during the imaging. In this case, an ROI, the spectral properties of which represent the leaf area, can be selected from one image only, and the spectral information of this region can be used to build a Spectral Library to be applied in the classification of other images as described above.

For comparison, in addition to classification done with the ENVI software, a 'visual classification' for subsets of pixels was also carried out. A pseudo-random subsample was obtained by selecting one using an 11×11 grid of pixels (every 10th pixel) in a warped visible image. These sample pixels were visually categorized, either as leaf or background, and compared with an automated classification for 10 separate images.

*Temperature analyses*: The classification results for the visible images were then used to extract corresponding temperatures from the thermal images. Using the ENVI Regions of Interest tool, a new region was created from the area classified as leaves. This region was overlaid on the thermal image, and the ENVI Statistics tool was used to calculate, for example, the mean temperature and the temperature distribution from this area. If needed, additional regions could also be selected for statistical analyses and the data exported for further analysis. For example, the areas with 'dry' reference leaves and 'wet' reference leaves could be separated from the visible image. Since the visible spectrum of these regions could not be separated from other leaf areas, the whole image was manually divided into different areas, containing the 'dry plant', the 'wet plant', and the experimental plant. These areas were then intersected with the region with the leaf area, and the statistics were calculated separately for each intersected region.

*Calculations: thermal indices*: Based on the temperature differences between the experimental plant, the 'dry plant', and the 'wet plant', the following thermal indices were calculated and used as a comparison with the measured stomatal conductance (Jones, 1999*a*):

$$CWSI=(T_{plant}-T_{wet})/(T_{dry}-T_{wet}) \quad (1)$$

$$I_G=(T_{dry}-T_{plant})/(T_{plant}-T_{wet}) \quad (2)$$

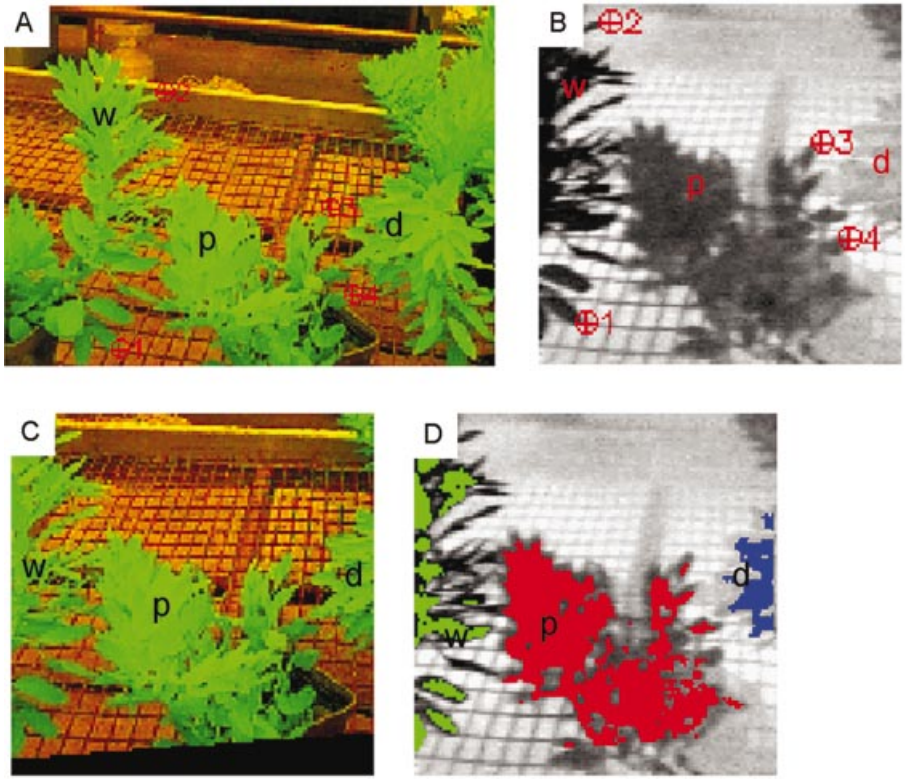


**Fig. 1.** An example of image processing of *Vicia faba* grown in a greenhouse. (A) An original visible image and Ground Control Points used in image overlaying, (B) corrected thermal image presented in a grey scale and Ground Control Points, (C) visible image warped and resampled to match the thermal image, and (D) classified leaf area overlaid with the thermal image and divided manually to represent the wet reference plant (green), experimental plant (red), and dry reference plant (blue). The results represent image processing where the value of 0.1 for the maximum vector angle parameter was used in the classification. The letter w indicates the wet reference plant, d the dry reference plant, and p the experimental plant.

where $T_{plant}$, $T_{dry}$, and $T_{wet}$ are the mean temperatures of the leaf area of the experimental plant, the dry reference plant, and the wet reference plant, respectively.

The index $I_G$ can also be expressed as follows (Jones *et al.*, 2002):

$$I_G = g_{lw}(r_{aW} + (s/\gamma)r_{HR}) \quad (3)$$

where $g_{lw}$ is the leaf conductance to water vapour transfer, $r_{aW}$ the boundary layer resistance to water vapour, $s$ the slope of the curve relating saturating water vapour pressure to temperature, $\gamma$ the psychrometric constant, and $r_{HR}$ the parallel resistance to heat and radiative transfer. According to equation (3), if other factors remain constant, the index $I_G$ is linearly related to the conductance (Jones, 1999*b*). As seen in equation (1), the index *CWSI* is linearly related to leaf temperature, in the case where the temperatures of the wet and dry references remain constant. These two indices are non-linearly related to each other and, therefore, the relationship between CWSI and stomatal conductance is also non-linear.

In order to evaluate the new method, the thermal indices were also calculated by applying the thresholding method developed earlier by Jones *et al.* (2002) (see above). Using the data from the greenhouse experiment, two threshold temperatures were determined from visually selected sample points from dry and wet reference plants in thermal images. All temperatures between these thresholds in the image were assumed to represent the temperature of the experimental plant. The mean temperature of this distribution, together with the wet and dry reference temperatures, were used to calculate the indices as described in equations (1) and (2).

## Results

An example of the image processing for the greenhouse data is presented in Fig. 1. The experimental plant is situated in the middle, the wet reference plant on the left, and the dry reference plant on the right. In the thermal image, the brightness of the grey scale represents the temperature. It can be seen that the wet reference is cooler than the experimental plant, while the dry reference is warmer. The background in the greenhouse situation was generally warmer than any of the plants.

The manually selected GCPs which are used in the warping of the visible image to produce Fig. 1C are shown in the images (Fig. 1A, B). The classification results are shown in Fig. 1D. Visual evaluation of the results indicates that, generally, the plants and the background are correctly separated. However, it can be seen that some parts of the actual leaf area are not classified as leaf. This area consists mainly of edge pixels, i.e. pixels that are mixed with the background. By increasing the maximum acceptable angle between vectors of the training class and any pixel to be classified (a parameter in the ENVI Spectral Angle Mapper classification pro-

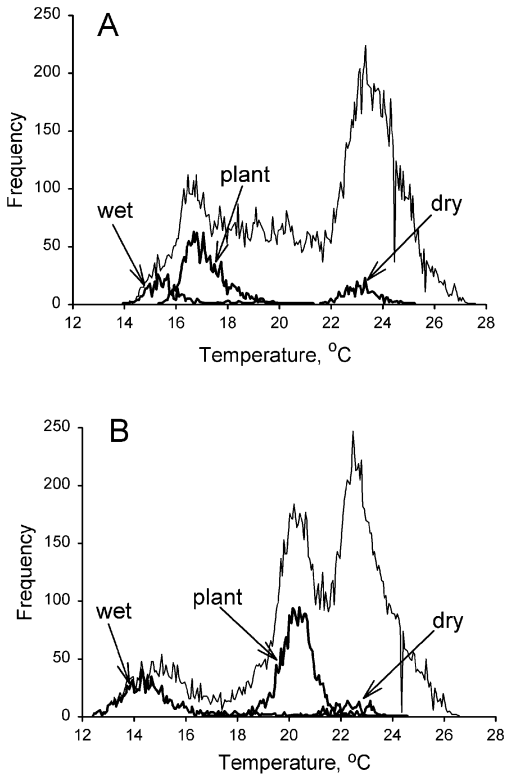


**Fig. 2.** Temperature distribution for a whole thermal image (thin line), and for a *Vicia faba* plant and dry and wet reference plants (thick lines), extracted from the image. (A) A well-watered plant and (B) a water-stressed plant.

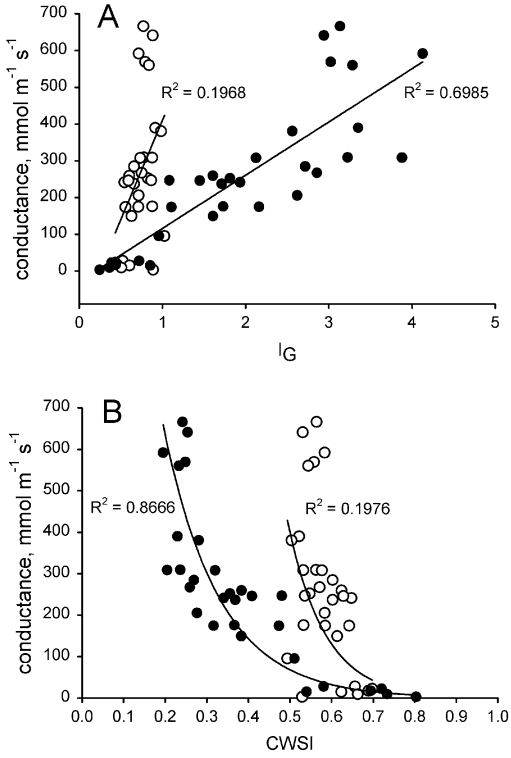


**Fig. 3.** The relationship between the measured stomatal conductance of *Vicia faba* and the calculated (A) linear thermal index $I_G$ and (B) non-linear thermal index *CWSI*. The results were calculated by using the Spectral Angle Mapper classification method with the maximum vector angle parameter set at 0.1 (closed symbols) and by using the method based on wet and dry temperature thresholds (open symbols).

**Table 1.** *Comparison of the results of the visual and automatic classification of the leaf area of* Vicia faba *with different values of the maximum vector angle parameter*

The percentage of actual leaf pixels (according to the visual classification) classified as leaves and the percentage of actual background pixels (according to the visual classification) classified as background by the ENVI classification. The results represent the mean over 10 separate images.

| | Maximum spectral angle | | | | | Number of pixels |
|---|---|---|---|---|---|---|
| | 0.05 | 0.1 | 0.2 | 0.3 | 0.4 | |
| Plant accuracy (%) | 36 | 57 | 76 | 90 | 96 | 425 |
| Background accuracy (%) | 98 | 98 | 96 | 95 | 92 | 785 |

cedure), more 'actual' (according to the visual classification) leaf pixels were classified as leaves, but on the other hand, more pixels visually classified as background were incorrectly classified as leaves by the automated classification (Table 1).

Figure 2 shows an example of the extracted temperature distributions for control and drought-stressed experimental plants, together with the dry and wet reference histograms in the greenhouse experiment. For comparison, the temperature distribution for the whole non-classified image (also including the background) is presented. This result shows that temperature distribution of the unclassified image includes two main peaks with some subsidiaries. The peaks with the lowest temperature consist mainly of the wet reference plant and the experimental plant, while the peak with the highest temperature consists mainly of background, the temperature of which is close to the temperature of the dry reference plant. By contrast, the results for the classified image clearly show single distributions with one peak for the experimental plant and for the dry and wet reference plants separately.

The effect of the value chosen for the maximum vector angle (used as a classification criterion in Spectral Angle Mapper; Table 1) on the temperature estimation is shown in Table 2. When the maximum accepted angle increases (more pixels are classified as plant), the calculated temperature for the experimental plant and the wet reference plant increase, while for the dry reference plant there is little effect. This effect probably arises because increasing the number of pixels classified as plant means that there are more mixed pixels, the temperature of which is partially affected by background. In the present study, the background temperature approximates that of the dry

reference and, therefore, the estimated dry reference temperature remains rather stable. The different effects on each component temperature (experimental plant, dry and wet references) mean that the selection of the classification parameters may affect the calculated thermal indices. Therefore, using a rather strict criterion for classification (small maximum vector angle) is probably the best choice, since this excludes most of the mixed pixels.

The relationships between stomatal conductance and the calculated thermal indices for *Vicia faba* are shown in Fig. 3. The linear correlation between conductance and $I_G$ and the non-linear relationship between conductance and *CWSI* were both in accordance with theory (equations (1)–(3), Jones, 1999*a*). In the same figure, the relationship between stomatal conductance and the thermal indices calculated using the method based on threshold temperatures (Jones *et al.*, 2002) is also presented. Compared with the automated classification method, the threshold method shows a much narrower range of the variation of calculated indices, a much steeper slope, and also weaker correlation with the conductance.

**Table 2.** *Effect of the value of the maximum vector angle parameter on the estimated plant temperature*

The mean temperatures calculated from 10 separate images of *Vicia faba*. The standard deviation of the 10 mean temperatures is shown in parenthesis.

| Maximum angle | Mean temperature (°C) | | |
|---|---|---|---|
| | Wet reference | Experimental plant | Dry reference |
| 0.05 | 15.6 (1.44) | 17.8 (1.57) | 22.9 (1.60) |
| 0.2 | 15.9 (1.36) | 18.0 (1.53) | 22.8 (1.66) |
| 0.4 | 16.5 (1.37) | 18.2 (1.47) | 22.8 (1.65) |

An example of the application of the method for determining shaded and sunlit canopy temperatures separately is presented in Fig. 4. In addition to the grapevine canopy, a complex filter paper reference including wet and dry sectors and two other references, together with a mounting tripod, are included in the image. In the classified image, three areas are separated. The area classified as sunlit canopy is shown as red, the shaded canopy as green and non-canopy areas as blue. Although the filter paper was recognized as non-canopy, much of the mounting was not correctly identified by the software.

Figure 5 shows temperature histograms for sunlit and shaded areas of the grapevine canopy for (A) the natural

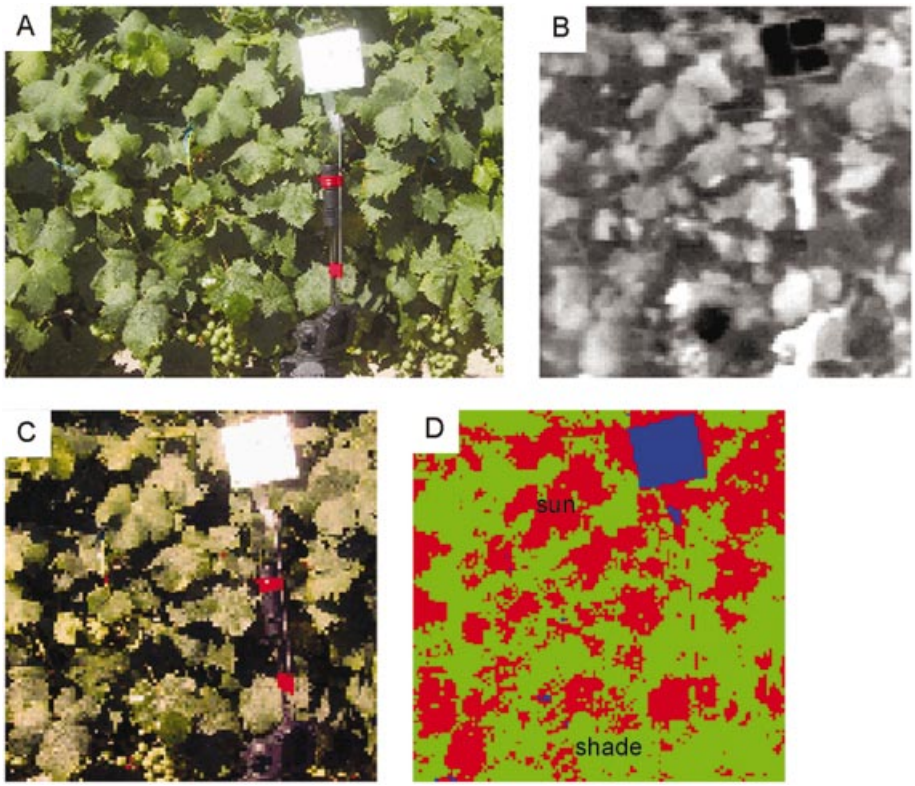


**Fig. 4.** An example of image processing to separate the shaded and sunlit leaves of of a grape-vine canopy (*Vitis vinifera* cv. Moscatel grown in field conditions, with natural rainfall treatment). (A) An original Red–Green–Blue visible image, (B) corrected thermal image presented in a grey scale, (C) visible image warped and cropped to match the thermal image, and (D) results of the classification of the warped visible image; red, classified as sunlit leaf area; green, classified as shaded leaf area; blue, classified as non-leaf area.

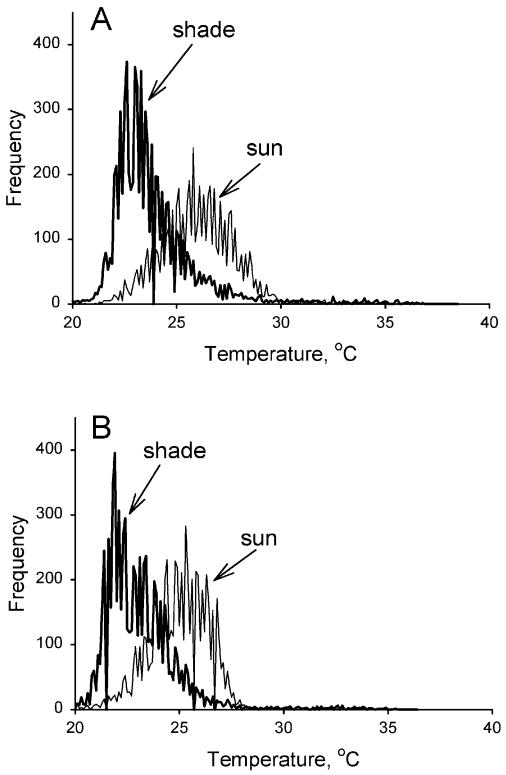


**Fig. 5.** Temperature distributions for shaded and sunlit leaves in *Vitis vinifera* (cv. Moscatel) canopies: (A) natural rainfall treatment and (B) fully irrigated treatment.

rainfall treatment, and (B) full irrigation. The mean temperatures and the corresponding standard deviations of the temperature distributions for sunlit and shaded areas for four replicate images from the fully irrigated and the natural rainfall treatments are shown in Fig. 6. Generally, the variance of the temperature in the shaded canopy was greater than in the sunlit canopy, and the natural rainfall treatment showed greater variance and higher temperatures than the full irrigation treatment.

## Discussion

Effective use of thermal imaging requires consistent, preferably automated, methods for analysing the images. This paper presents a method based on the parallel use of thermal and visible images to measure the temperature variation of whole plants and, further, to estimate stomatal conductance in a non-contact manner. It is based on the development of automated approaches to the identification of areas of interest, *independently* of the thermal image itself, by the use of image analysis on either R/NIR or RGB digital images. The methods used here for image processing have been developed for, and are widely used in, remote sensing (Campbell, 1996; Mather, 1999), but rarely in small-scale ecological studies (Corp *et al.*, 2003; Schuerger *et al.*, 2003).

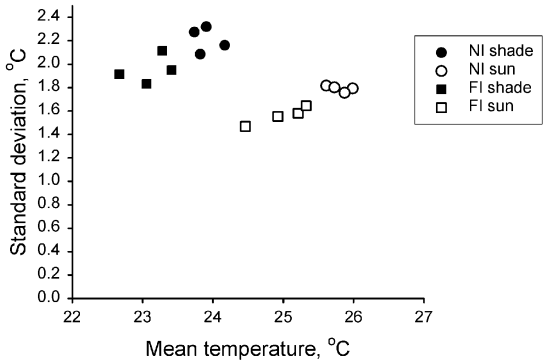


**Fig. 6.** The mean temperatures and standard deviations of temperature distributions for four replicate images from shaded and sunlit *Vitis vinifera* canopy from natural rainfall (NI) and fully irrigated (FI) treatments.

The accuracy of the resulting temperature distribution depends on two critical steps: (i) the overlaying of the thermal and visible images, and (ii) the classification of the visible image. For overlaying, the selection of the GCPs is particularly time-consuming, but if the same GCPs can be used for several images, such as in a robotic analysis system (Chaerle *et al.*, 2003), the image processing would be much more flexible. This requires, however, that the position of both cameras would be exactly the same when each image is taken. An alternative approach would be to have a rigid mounting system for the cameras, where the geometry is fixed, so a standard overlaying algorithm that would correct for differences in view angle and field of view could be applied in all situations.

The accuracy of classification depends on identifying all those pixels the spectral properties of which are close enough (according to predefined criteria) to areas that are known to represent the object of interest, in this case, green leaves. The choice of classification method and criteria vary depending on both the camera wavebands used (R/NIR or RGB) and on the properties of the objects included in the image and the purpose of image processing, and should be tested for any particular combination of canopy and vegetation studied. In this study, two separate classification methods were used, Spectral Angle Mapper and Minimum Distance; both were effective for the glasshouse and the field study (R/NIR and RGB images, respectively). The main difference between these methods is whether the brightness of the pixels is used as the classification criterion or not. In the case where the total leaf area of plants is used to determine the temperature distribution, brightness as a criterion is unnecessary and may cause the incorrect exclusion of some of the leaves. By contrast, where one aims to separate sunlit and shaded leaves, the brightness is essential.

A key interest is to determine how this automated image analysis compares with alternative methods for separation of areas of interest. Manual selection (Jones *et al.*, 2003) is

slow and subjective, while the use of background material, the temperature of which differs from that of the objects of interest (Guiliani and Flore, 2000; Pearce and Fuller, 2001), is not always possible or very practical, especially in field conditions. The use of wet and dry reference surfaces as thresholds to determine limits of the canopy temperature distribution has been proposed by Jones *et al.* (2002). One problem, however, is that if the temperature of the experimental plant is close to the temperature of either the wet or dry reference, i.e. in cases with either very open or very closed stomata, the temperature distributions of the experimental plant and the wet or dry references unavoidably overlap. In such cases, bias can arise as some reference pixels are included and some plant pixels are excluded.

Furthermore, in some cases the selection of leaf area on the basis of reference thresholds alone may lead to inclusion of objects other than leaves (e.g. stems or ground), again potentially biasing the results. In the greenhouse experiment of the present study, the temperature of the dry reference leaves was very close to the background temperature. Therefore, the use of wet and dry threshold temperatures led to the inclusion of substantial background so that the differences of the actual plant temperature between water-stressed and non-water-stressed conditions were underestimated. In addition, the temperature distribution of the experimental plant, estimated by the threshold method, moved towards the temperature of the dry reference. These effects together had a major and substantial effect on the relationships between stomatal conductance and either CWSI or $I_G$ (Fig. 3) leading to the threshold method overestimating the true gradient of the relationship between $I_G$ and conductance, as assessed against the pixel classification method.

The criteria determining inclusion of pixels in a certain class also substantially affect the outcome of the thermal analysis (Table 2). The use of a strict classification excludes most of the mixed pixels from the thermal image and reduces the effect of background in the thermal analyses, even though some of the actual leaf area may also be excluded. The proportion of mixed pixels depends on the resolution of the thermal image (to which resolution the visible image is resampled). The use of high resolution thermal imagers, which, though more expensive, are becoming more widely available, reduces the relative proportion of mixed pixels and allows more effective utilization of the thermal data.

An important application of image analysis is the separation of shaded and sunlit parts of the canopy (Ewing and Horton, 1999; Jones and Leinonen, 2003). In an earlier study (Jones *et al.*, 2002) the temperatures of the shaded and sunlit grapevine canopy components were estimated by manually selecting corresponding large areas from shaded and sunlit sides of a canopy. In that case, the greater temperature variance for the sunlit side probably largely arose because of the substantial fraction of shaded leaves visible on the sunlit side. The present method is based on the classification of the image pixel by pixel, so it has potential to improve greatly the accuracy of calculating the temperature distribution for the sunlit and shaded leaves separately, as can be seen in Fig. 5.

By contrast with the earlier study (Jones *et al.*, 2002), the present results show that the temperature variance of the sunlit leaves (as opposed to the sunlit side of the canopy) is not higher, but actually lower, than that of the shaded leaves. Although this does not appear to support the idea (Fuchs, 1990), that the variability in leaf orientation causes more variation in the leaf energy balance and temperature in the sunlit than the shaded leaves, this result may be related to two factors: (i) the leaf angle distribution is not random for these canopies (see, for example, Fig. 4), and (ii) the stomata are more closed in the shaded parts of the canopy compared with the sunlit part (Jones *et al.*, 2002; de Souza *et al.*, 2003), thus tending to increase the variance in the shade (Fuchs, 1990). The present results are, therefore, entirely consistent with Fuchs' idea that temperature variation increases as stomata close (Fuchs, 1990); indeed the clear tendency for temperature and variance to be greater for NI than for FI treatments (Fig. 6) correlates well with the higher conductance observed for the FI vines (Jones *et al.*, 2002; de Souza *et al.*, 2003). More empirical data are needed to verify these results, but it is possible that the temperature variation itself, in addition to the absolute temperature, may become a useful index for estimation of the stomatal conductance in field conditions.

In conclusion, the partly automated image processing method presented in this study provides new applications for thermal imaging in plant-stress studies. Compared with earlier methods, the present method allows more accurate determination of the thermal indices, which can be used to estimate the level of stomatal conductance in the plant canopy. Furthermore, the accurate separation of sunlit and shaded parts of a canopy makes it possible to study the possibilities of using temperature variation as an indicator of stomatal conductance and plant stress.

## Acknowledgements

Ilkka Leinonen acknowledges the financial support provided through the European Community's Human Potential Programme under contract HPRN-CT-2002-00254 (STRESSIMAGING). We are also very grateful for funding under EU Framework 5 project IRRISPLIT (ICA3-CT-1999-00008) and to Professor Manuela Chaves and colleagues for access to the experiments at Pegões.

## References

**Campbell JB.** 1996. *Introduction to remote sensing*, 2nd edn. London: Taylor and Francis.

**Chaerle L, Hulsen K, Hermans C, Strasser RJ, Valcke R, Hofte M, Van Der Straeten D.** 2003. Robotized time-lapse imaging to assess *in planta* uptake of phenylurea herbicides and their microbial degradation. *Physiologia Plantarum* **118,** 613–619.

**Corp LA, McMurtrey JE, Middleton EM, Mulchi CL, Chappelle EW, Daughtry CST.** 2003. Fluorescence sensing system: *in vivo* detection of biophysical variations in field corn due to nitrogen supply. *Remote Sensing of Environment* **86,** 470–479.

**de Souza CR, Maroco JP, dos Santos TP, Rodrigues ML, Lopes CM, Pereira JS, Chaves MM.** 2003. Partial rootzone drying: regulation of stomatal aperture and carbon assimilation in field-grown grapevines (*Vitis vinifera* cv. Moscatel). *Functional Plant Biology* **30,** 653–652.

**Ewing RP, Horton R.** 1999. Quantitative color image analysis of agricultural images. *Agronomy Journal* **91,** 148–153.

**Fuchs M.** 1990. Infrared measurement of canopy temperature and detection of plant water stress. *Theoretical and Applied Climatology* **42,** 253–261.

**Guiliani R, Flore JA.** 2000. Potential use of infrared thermometry for the detection of water stress in apple trees. *Acta Horticulturae* **537,** 383–392.

**Idso SB.** 1982. Non-water-stressed baselines: a key to measuring and interpreting plant water stress. *Agricultural Meteorology* **27,** 59–70.

**Idso SB, Jackson RD, Pinter PJ, Reginato RJ, Hatfield JL.** 1981. Normalizing the stress-degree-day parameter for environmental variability. *Agricultural Meteorology* **24,** 45–55.

**Jackson RD.** 1982. Canopy temperature and crop water stress. *Advances in Irrigation Research* **1,** 43–85.

**Jones HG.** 1992. *Plants and microclimate*, 2nd edn. Cambridge: Cambridge University Press.

**Jones HG.** 1999*a*. Use of infrared thermometry for estimation of stomatal conductance as a possible aid to irrigation scheduling. *Agricultural and Forest Meteorology* **95,** 139–149.

**Jones HG.** 1999*b*. Use of thermography for quantitative studies of spatial and temporal variation of stomatal conductance over leaf surfaces. *Plant, Cell and Environment* **22,** 1043–1055.

**Jones HG, Aikman DA, McBurney T.** 1997. Improvements to infrared thermometry for irrigation scheduling. *Acta Horticulturae* **449,** 259–266.

**Jones HG, Leinonen I.** 2003. Thermal imaging for the study of plant water relations. *Journal of Agricultural Meteorology* **59,** 205–217.

**Jones HG, Stoll M, Santos T, de Sousa C, Chaves MM, Grant OM.** 2002. Use of infrared thermography for monitoring stomatal closure in the field: application to grapevine. *Journal of Experimental Botany* **53,** 2249–2260.

**Lillesand TS, Kiefer RW, Chipman JW.** 2004. *Remote sensing and image interpretation*, 5th edn. New York: John Wiley and Sons Inc.

**Mather P.** 1999. *Computer processing of remotely-sensed images: an introduction*. Chichester: John Wiley.

**Merlot S, Mustilli A-C, Genty B, North H, Lefebvre V, Sotta B, Vavasseur A, Giraudat J.** 2002. Use of infrared thermal imaging to isolate *Arabidopsis* mutants defective in stomatal regulation. *The Plant Journal* **30,** 601–609.

**Pearce RS, Fuller MP.** 2001. Freezing of barley studied by infrared video thermography. *Plant Physiology* **125,** 227–240.

**Schuerger AC, Capelle GA, Di Benedetto JA, Mao C, Thai CN, Evans MD, Richards JT, Blank TA, Stryjewski EC.** 2003. Comparison of two hyperspectral imaging and two laser-induced fluorescence instruments for the detection of zinc stress and chlorophyll concentration in bahia grass (*Paspalum notatum* Flugge). *Remote Sensing of Environment* **84,** 572–588.

**Webb N.** (ed.) 1990. *AP4 porometer user manual.* Cambridge, England: Delta-T Devices Ltd.